ORIGINAL ARTICLE

CrossMark

# New hybrid composites for photodynamic therapy: synthesis, characterization and biological study

N. Kutsevol[1] · A. Naumenko[1] · Yu. Harahuts[1] · V. Chumachenko[1] · I. Shton[2] · E. Shishko[2] · N. Lukianova[2] · V. Chekhun[2]

## Abstract

Photodynamic therapy is a procedure that uses a photosensitizing drug to apply light therapy selectively to target cancer treatment. This study is focused on a synthesis and characterization of a new hybrid nanocomposites based on the branched copolymers dextran–polyacrylamide in nonionic, D-g-PAA and anionic D-g-PAA(PE) form, with incorporated gold nanoparticles (AuNPs) and photosensitizer chlorin e6 (Ce6) simultaneously. Double polymer/AuNPs and trial polymer/AuNPs/Ce6 were studied by TEM, UV–visible, SOSG fluorescence. It was found the drastic difference for absorbance for trial nanosystems synthesized in nonionic and anionic polymers matrices. It was established that for the nanocomposite synthesised in anionic polymer matrix with the Ce6:Au mass ratio 1:10 generation of singlet oxygen ($^1O_2$) was quite close to that for free Ce6. The study of ability of this nanosystem to sensitize MT-4 cells to photodynamic damage has shown that the nanocomposite, that contained AuNPs during the synthesis of which $HAuCl_4$:$NaBH_4$ mass ratio was 1:2 showed higher photodynamic activity, than Ce6 itself. Nanosystem D70-g-PAA(PE)/AuNPs/Ce6 can be recommended to experiment in vivo.

**Keywords** Nanocomposite · Star-like copolymer · Gold nanoparticle · Photosensitizer · Photodynamic activity

## Introduction

Photodynamic therapy (PDT) is being recognized as alternative treatment for cancer therapy. This treatment is based on two procedures: the use of a photosensitive drug and illumination of the tumor to activate photosensitizer (Liu et al. 2017). Efficacy of PDT is high for small superficial tumors without long-term side effects. The procedure can be repeated without cumulative toxicity (Triesscheijn et al. 2006; Castano et al. 2004).

The first clinical application of PDT was described in 1903 (Triesscheijn et al. 2006). However, it took another 70 years, before the PDT for the treatment in oncology became widely used. In 1975, Dougherty et al. (1977, 1978) reported that hematoporphyrin derivative in combination with red light could completely eradicate mouse mammary tumor growth. Following these successful treatments, numerous studies have been done involving a variety of cancers and photosensitizers.

The efficacy of PDT depends on few factors: the type of photosensitizer, drug concentration, its tumor accumulation efficacy, light dose, and oxygen availability (Xing et al. 2016; Abbas et al. 2017; Yang et al. 2016; Zhang et al. 2016; Song et al. 2017). Singlet oxygen generated by the photochemical reaction can directly kill tumor cells by the induction of apoptosis and necrosis (Bauer 2016, 2017; Riethmuller et al. 2015).

A modern trend in PDT is the use of multifunctional polymer nanocarrier which can enhance target-oriented PDT. The polymer nanocarriers can be of few types: liner- and branched polymers, dendrimers, micelles, and nanogels (Wang and Rempel 2015; Shroff and Vidyasagar 2013). Our previous study has shown that branched star-like carboxylate containing polymers could be efficient nanocarriers for drug delivery to tumor cells (Charrueau and Zandanel 2016) and can be efficient matrices for gold nanoparticle preparation in water medium (Yeshchenko et al. 2016). The theoretical (Merlitz et al. 2011; Everaers et al. 2017; Kutsevol et al. 2015) and experimental studies (Boué et al. 2016; Solano-Umaña and Vega-Baudrit 2015) of star-like

✉ A. Naumenko
a_naumenko@univ.kiev.ua

1 Taras Shevchenko National University of Kyiv, Volodymyrska, 60, Kiev 01601, Ukraine

2 R.E. Kavetsky Institute for Experimental Pathology, Oncology and Radiobiology, Vasilkivska, 45, Kiev 03022, Ukraine

Springer
مدينة الملك عبدالعزيز للعلوم والتقنية KACST

polymers provided that branched macromolecules have a higher local concentration of functional groups capable of reacting with drugs or other substances which can be incorporated into polymer nanocarrier. The use of hybrid nanosystems consisting of polymer nanocarrier with incorporated plasmonic metal nanoparticles and photosensitizer seems to be the most efficient approach for PDT treatment in oncology. Desired metal nanostructures for biomedical use should have strong and tunable surface plasmon resonance (SPR), low toxicity, ease of delivery, and convenience for bioconjugation for actively targeting cancer cells. Gold nanoparticles (AuNPs) with controlled geometrical, optical, and surface chemical properties are the subject of intensive studies and applications in cancer diagnosis, cancer therapy, etc. (Cai et al. 2008; Chithrani et al. 2010).

The goal of this study was to create hybrid nanocarriers based on the branched copolymers dextran–polyacrylamide in nonionic and anionic from with incorporated AuNPs and photosensitizer, to characterize this system and to test their biological activity as the nanocomposites for PDT.

## Materials and methods

### Reagents

Tetrachloroauric acid, sodium borohydride were purchased from Sigma-Aldrich (USA) and used without further purification.

Fetal bovine serum (FBS), Hank's balanced salt solution (HBSS) without phenol red and RPMI-1640 were obtained from Sigma-Aldrich (USA), photosensitizer chlorin e6 (Ce6) was obtained from Santa Cruz Biotechnology (USA). Singlet oxygen sensor green (SOSG) was obtained from Molecular Probes (USA). Dimethyl sulfoxide (DMSO) was obtained from Serva (Germany).

### Polymer nanocarrier

Copolymers dextran-graft-polyacrylamide (D-$g$-PAA) with dextran core ($M_w = 70 \times 10^5$ g/mol) and five grafted PAA chains in nonionic and anionic form were used as a polymer matrix for AuNPs synthesis and fabrication of trial nanosystems containing gold nanoparticles (AuNPs) and photosensitizer chlorin e6 (Cle6) simultaneously. Synthesis, molecular parameters and peculiarities of macromolecular structure of star-like copolymer D-$g$-PAA were discussed in details in Kutsevol et al. (2012). The average molecular weight of D-$g$-PAA ($M_w$) was equal to $1.57 \times 10^6$ g/mol, radius of gyration ($R_g$)—67 nm, and polydispersity ($M_w/M_n$)—1.81.

Anionic form of the copolymer (referred throughout as D-$g$-PAA(PE)) was obtained via alkaline hydrolysis of initial copolymer during 30 min using sodium hydroxide. The fraction of MERS bearing carboxylate groups evaluated by potentiometric titration was equal to approximately 37% (Kutsevol et al. 2014). The D-$g$-PAA(PE) copolymer was purified, freeze-dried and kept under vacuum for preventing them from further hydrolysis.

## Gold nanoparticles synthesis

The AuNPs were synthesized by the chemical reduction of Au precursor (tetrachloroauric acid). All synthesized polymers play a role of matrices capable to act as nucleating, capping and stabilizing agents simultaneously.

0.012 ml tetrachloroauric acid aqueous solution ($C = 0.1$ M) was added to 0.5 ml of aqueous polymer solution ($C = 1 \times 10^{-3}$ g/cm$^3$) and stirred during 20 min. Then, 0.047 ml of 0.1 M aqueous solution of sodium borohydride was added. The final solution was stirred for 30 min. It turned ruby red in color, thus the formation of Au NPs was indicated. The reduction process was performed at $T = 25$ °C.

## Synthesis of hybrid nanosystem polymer/AuNO$_3$/Ce6

All polymer/AuNPs composites with Ce6 were prepared ex tempore. Stock solution of Ce6 (1 mg/ml) was prepared in DMSO. Then, photosensitizer solution was 100-fold diluted in HBSS with constant stirring. The resulting Ce6 solution was gently mixed with D-$g$-PAA(PE)/AuNPs or D-$g$-PAA(PE) and incubated in room temperature for 5 min before use.

## UV–visible spectroscopy

UV–visible absorption spectra of silver sols were recorded by UV–visible spectrophotometer UV1900 from 200 to 800 nm.

## Transmission electron microscopy (TEM)

For the sample preparation 400 mesh Cu grids with plain carbon film were rendered hydrophilic by a glow discharge treatment (Elmo, Cordouan Technologies Bordeaux France). A 5 µl drop was deposited and let adsorbed for 1 min, then the excess of solution was removed with a piece of filter paper. The observations of the AgNPs were carried out employing two TEMs, Tecnai G2 or CM12 (FEI, Eindhoven Netherlands) and the images were acquired with a ssCCD Eagle camera on the Tecnai and a Megaview SIS Camera on the CM12.

## Singlet oxygen registration

Singlet oxygen ($^1O_2$) formation was monitored using SOSG. Test solutions were prepared in TRIS buffer (pH 7.4). Stock solution of fluorescent reagent SOSG in methanol (5 mM) was prepared and stored at $-20$ °C before use, following the manufacturer's instructions. For the registration of $^1O_2$ generation level by Ce6 and its nanocomposites with polymer/AuNPs upon laser irradiation 2 µM of SOSG was added to each sample. The probes were irradiated by semiconductor laser (Photonica Plus, Ukraine; $\lambda = 658$ nm) fractionally up to a dose of 2 J/cm$^2$. SOSG fluorescence at 530 nm was registered using fluorospectrometer NanoDrop 3300 (NanoDrop, USA).

## Cell cultures

The MT-4 cells (human T cell leukemia) were obtained from the Bank of Cell Lines from Human and Animal Tissue of the R.E. Kavetsky Institute for Experimental Pathology, Oncology and Radiobiology of the National Academy of Sciences of Ukraine. Cells were maintained in RPMI-1640 containing 10% FBS at 37 °C in humidified atmosphere and 5% $CO_2$.

## Cell survival assay (MTT-test)

The *evaluation of dark cytotoxicity* of nanoparticles and nanocomposites was carried out by serial dilutions. Calculation of live/dead cells was determined after their staining with trypan blue, and cell viability using MTT test.

The basis of the method is the ability to convert 3-[4,5-dimethylthiazole-2-1]-2,5 diphenyltetrazolium bromide—yellow salt to crystalline MTT-formazan of purple color using the mitochondrial enzymes of the living cell. To this end, 20 µl of MTT solution (Sigma, USA) (stock solution—5 mg/ml in phosphate buffer) was added to the wells of a 96-well plate with initial and molding resistance, and incubated under the same conditions for 3 h After centrifugation of the plate with cells (1500 rpm, 5 min), the supernatant was removed. To dissolve the formazan crystals in each well, 100 µl of dimethyl sulfoxide (Serva, Germany) was added. The optical absorption of the solution was measured using a multi-spectrophotometer ("STAT FAX 2100") at a wavelength of 540 nm.

## Photodynamic therapy

For PDT, cell suspensions ($0.5 \times 10^6$ per ml) in HBSS were prepared from a culture of the leukemic cell line in a log phase of growth. After 1.5 h of incubation (37 °C) in HBSS with Ce6 alone (0.1 mkg/ml) or with D-$g$-PAA(PE)/AuNPs/Ce6 nanocomposite containing the same concentration of photosensitizer (Ce6:Au mass ratio 1:10), the cells were washed twice with a 10-fold volume of fresh HBSS and were exposed to the red (658 nm) laser light (power density 1.1 mW/cm$^2$, dose 1 J/cm$^2$). After irradiation, the cells were transferred to growth medium and incubated at 37 °C for 18 h to complete photodynamic-induced apoptosis process. Cell viability was determined by trypan blue dye exclusion test or by MTT-test.

## Results and discussion

Both sols synthesized in solutions of nonionic and anionic branched polymer were stable in time (with out any precipitation). Should be noted that attempt to synthesized stable Au sol in anionic linear PAA matrix was not successful, the precipitate was observe just after synthesis. The same results was describe for Ag sols obtained in anionic linear PAA (Kutsevol et al. 2015). TEM images of AuNPs, synthesized in the solution of D70-$g$-PAA and D70-$g$-PAA(PE) are represented in Fig. 1.

It is seen that sols synthesized in nonionic and anionic polymer matrices differ in size characteristics of AuNPs. Nanosystem obtained in nonionic polymer matrix contains individual nanoparticles of 1.5–2 nm in size (Fig. 1c) and some clasters of nanoparticles (Fig. 1a). Should be noted that size of nanoclasters corresponds to size of individual polymer molecule in solution (50–60 nm). The well-defined clasters are not observed for sol synthesized in anionic polymer solution (Fig. 1b). AuNPs synthesized into D70-$g$-PAA(PE) solutions are of 2–10 nm in size (Fig. 1c) and this nanosystem is more monodispersed in comparison with one prepared in nonionic matrix.

UV–visible spectroscopy has been used for characterization of trial nanosystems D70-$g$-PAA/AuNPs/Ce6 and D70-$g$-PAA(PE)/AuNPs/Ce6 regarding the efficient composition for PDT. The first stage was study of dual nanosystems systems: D70-$g$-PAA/AuNPs and D70-$g$-PAA(PE); D70-$g$-PAA/Ce6 and D70-$g$-PAA(PE)/Ce6.

UV–visible spectra of AuNPs synthesized in solutions of star-like D70-$g$-PAA and D70-$g$-PAA(PE) polymers are shown in Fig. 2. Well-defined surface plasmon resonance (SPR) for gold nanoparticles was observed for all prepared sols. It is evident the difference in absorption curves for sols synthesized in nonionic and anionic star-like polymer matrices. The intensity of SPR band is higher for nanosystem D70-$g$-PAA(PE). In addition, the SPR band is more extended for this nanosystem.

The absorption spectrum of chlorine e6 (Ce6) solutions in the nonionic and anionic polymer is shown in Fig. 3. The most intense band (Sore band absorption with maxima at 405 nm) is located in near UV range, while the Q bands (504 and 650 nm) are located in red section of the spectrum. The
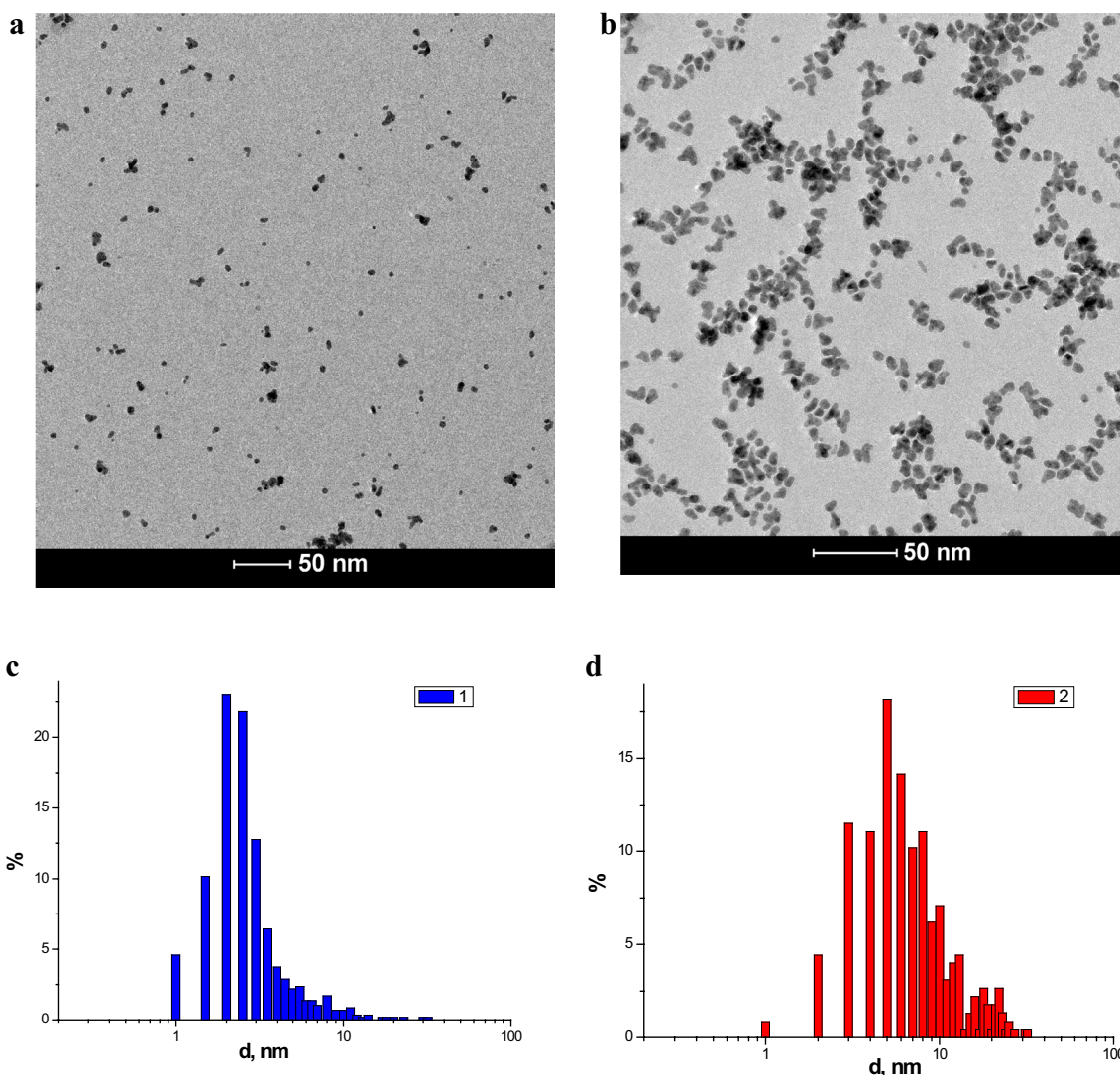
**Fig. 1** TEM images (**a**, **b**) and size nanoparticle distribution (**c**, **d**) in Au sols synthesized in D70-*g*-PAA (**a**, **c**) and D70-*g*-PAA (PE) solutions (**b**, **d**)

experimentally registered spectrum confirms the literature data (Zenkevich et al. 1996; Gladkova et al. 2010; http://omlc.ogi.edu/spectra/PhotochemCAD/html/141.html).

Absorption spectra of the triple system "polymer/gold nanoparticles/photosensitizer" are shown in Fig. 4. Comparative analysis of the spectra for dual polymer/AuNPs nanosystem (Fig. 2), dual nanosystem polymer/Ce6 (Fig. 3) and trial polymer/AuNPs/Ce6 nanosystems (Fig. 4) allows to conclude: a peak 1 corresponds to a sore band (400 nm), peak 2 (Q-band in the region of 660 nm)—to a photosensitizer; a peak 3 (530 nm) is SPR of gold nanoscale particles. Both types of polymer matrices do not absorb in this range of wavelengths.

It is evident that contributions of components of the triple system to the absorption of nanosystems are not additive (Figs. 2, 3, 4). It is the mostly expressed in the

region of SPR of AuNPs. The SPR band for triple nanosystems becomes more expanded; the intensity of absorption decreases in comparison with dual nanosystems. It testified the existence of the interaction of the photosensitizer chlorine e6 with AuNPs.

Figure 5a demonstrates changes in spectra for trial nanosystem D-*g*-PAA/AuNPs/Ce6 by varying the concentration of AuNPs. Decrease in the intensity and blue shift (to 5 nm) of the sore band are observed. The Q-band is gradually overlapping with the SPR band in the region of 530–540 nm. The most significant changes occur for the Q-band (maximum absorption at 650 nm). The decrease of intensity as well as division into two bands (maxima ~ 620 nm, and ~ 705 nm) are observed. These two maxima become more pronounced with further increase in AuNP concentration.
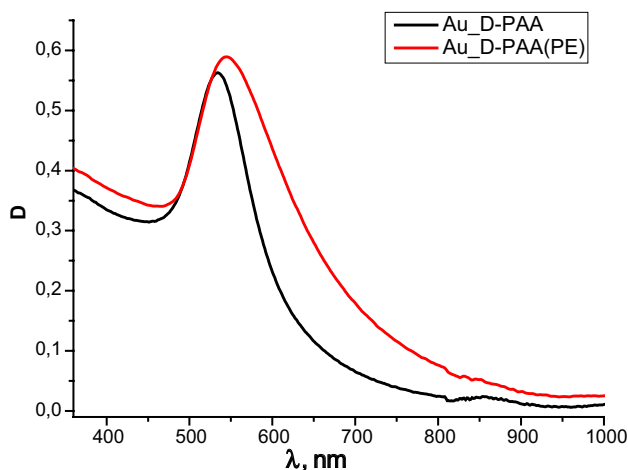
**Fig. 2** Absorption spectra of nanosystems: D70-*g*-PAA/AuNPs (black curve); D70-*g*-PAA(PE)/AuNPs (red curve)
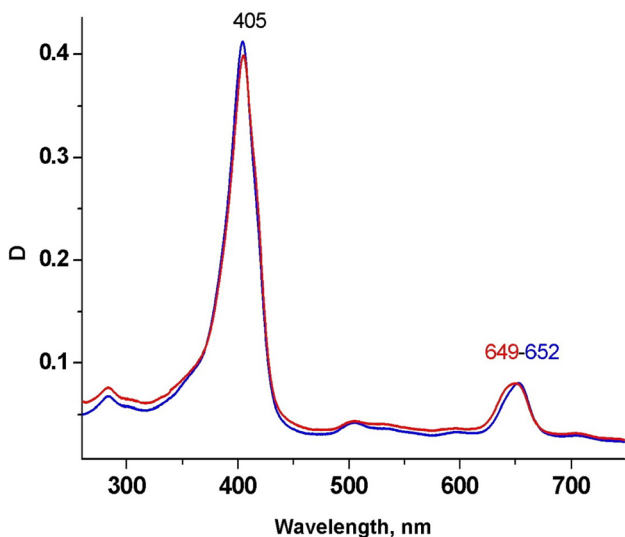


**Fig. 3** Absorption spectra of system: D70-*g*-PAA/Ce6 (red curve); D70-*g*-PAA(PE)/Ce6 (blue curve)



**Fig. 4** UV–visible spectra of triple nanosystems: D70-*g*-PAA/AuNPs/Ce6 (red curve); D70-*g*-PAA(PE)/AgNPs/Ce6 (blue curve), $C_{\text{AuNPs}} = 5$ mkl

Figure 5b demonstrates changes in spectra for trial nanosystem D70-*g*-PAA(PE)/AuNPs/Ce6 at different AuNPs concentration. One can see that in the case of ionic matrices the individual character of photosensitizer spectra persists longer. To illustrate this fact, we built the dependences of the intensities of character spectral bands from the concentration of golden nanoparticles. Such dependences for sore band (405 nm) on the AuNPs concentration for D70-*g*-PAA/AuNPs/Ce6 and D70-*g*-PAA(PE)/AuNPs/Ce6 trial nanosystems are shown in Fig. 6. One can see that the efficiency of Ce6 decreases more slowly with increase of AuNP concentration for nanosystem synthesized in anionic polymer matrix in comparison with nonionic one.
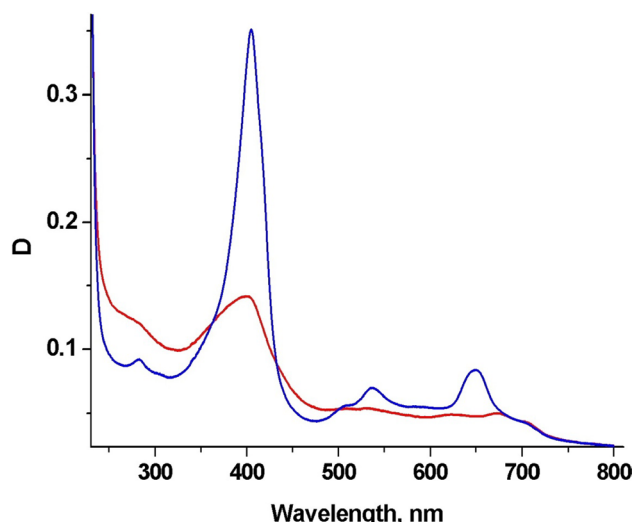
It is seen in (Fig. 6) that the optimal concentration of AuNPs exists when the drastic difference for absorbance for trial nanosystems synthesized in nonionic and anionic polymer matrices reveal. From Fig. 4 that represents the absorbance of trial nanosystems synthesised both polymer matrix at the same concentration of AuNPs it is also evident that nanosystem D-*g*-PAA(PE)/AuNPs/Ce6 is more efficient and can be used in the more wide region of the AuNP concentration. Thus, namely this nanosystem was proposed for biological test, since the better photodynamic result can be expected.

Analyzing the singlet oxygen generation by D-*g*-PAA(PE)/AuNPs and their composites with Ce6 we observed its gradual decrease with the rise of Au content in nanocomposites for all doses of laser irradiation applied (Fig. 7). It can be speculated, that AuNPs are able to quench the singlet oxygen generation by photosensitizer upon their contact in the composite. Nevertheless, with the Ce6:Au mass ratio 1:10 $^1O_2$ generation was quite close to that for free Ce6. It is should be noted that, in samples containing D-*g*-PAA(PE)/AuNPs or polymer alone without photosensitizer, no singlet oxygen production was registered.

Since D-*g*-PAA(PE)/AuNPs/Ce6 upon laser irradiation was able to produce the main cytotoxic component for photodynamic therapy—singlet oxygen—we tested the ability of this nanosystem to sensitize MT-4 cells to photodynamic damage. One of the most important parameters for the effectiveness of nanocomposite photosensitizers is the interaction of the dye molecule with the nanocarrier. Even minor changes in the conditions of its synthesis can dramatically affect the final result. Therefore, we decided to study how the mass ratio of tetrachloroauric acid to sodium borohydride,
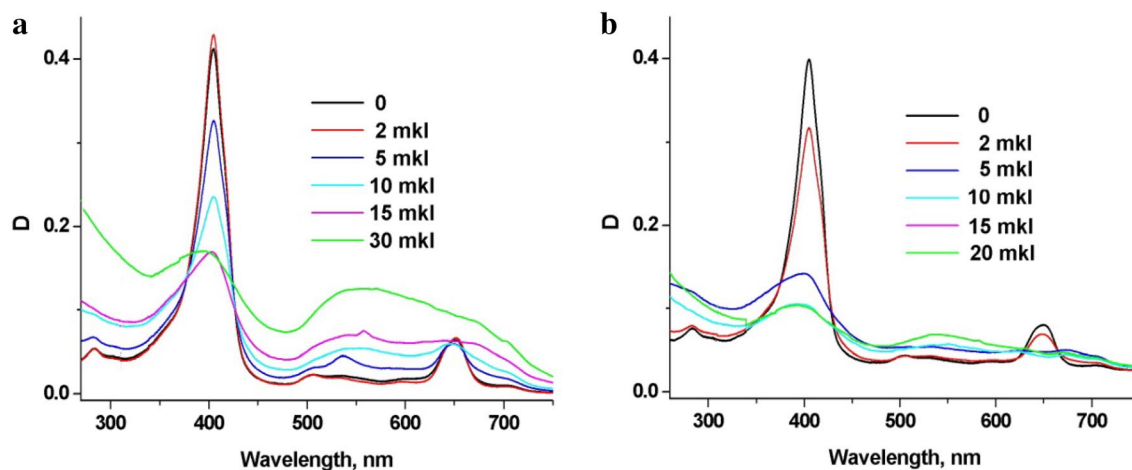
**Fig. 5** Absorption spectra of trial system D70-*g*-PAA/AuNPs/Ce6 (**a**) and D70-*g*-PAA/AuNPs/Ce6 (**b**) at various AuNPs concentration
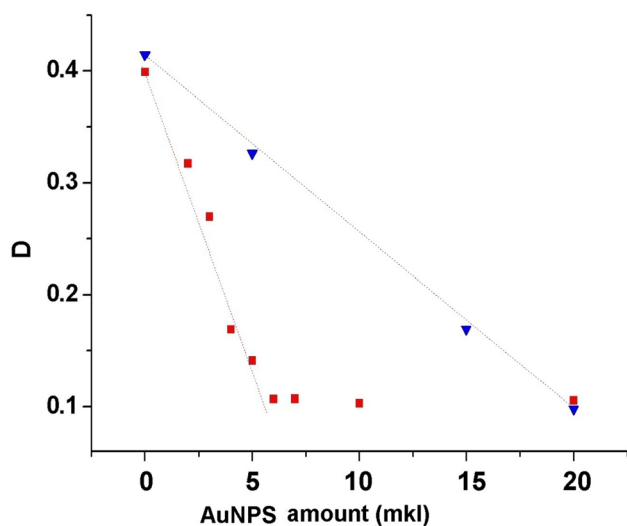


**Fig. 6** Dependence of optical density of sore band on the AuNPs concentration for D70-*g*-PAA/AuNPs/Ce6 (red curve) and D70-*g*-PAA(PE)/AuNPs/Ce6 (blue curve) trial nanosystems



**Fig. 7** Singlet oxygen generation by D-*g*-PAA(PE)/AuNPs/Ce6 nanosystems with different Ce6:Au mass ratio

which was used as a reducing agent in the synthesis of AuNPs, affects the resulting photodynamic activity of D-*g*-PAA(PE)/AuNPs/Ce6 nanocomposite photosensitizers. The mass ratio of Ce6:Au in all tested samples was 1:10. And the concentration of Ce6 in all probes was equal to 0.1 μg/ml. As a result, nanocomposite, that contained AuNPs during the synthesis of which $HAuCl_4$:$NaBH_4$ mass ratio was 1:2 showed higher photodynamic activity, than Ce6 itself (Fig. 8). Interestingly, the increase of $NaBH_4$ concentration during nanoparticles synthesis lead to decrease of the whole D-*g*-PAA(PE)/AuNPs/Ce6 nanocomposite activity to the level of free photosensitizer. This may indicate the exceptional importance of ionic interactions in the nanosystem, as
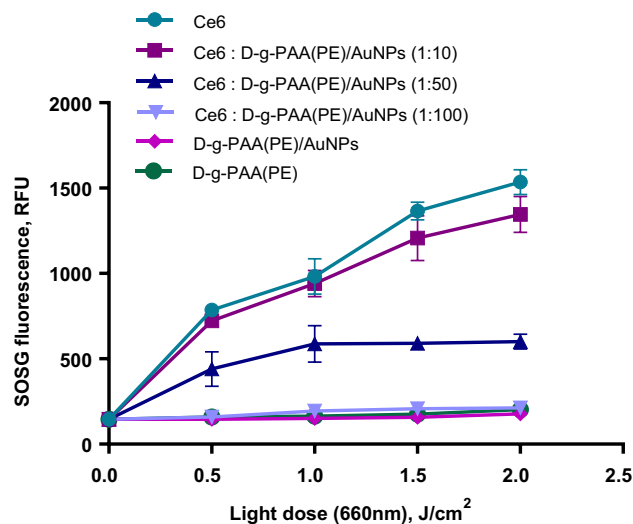
residual quantities of sodium borohydride may hamper the negatively charged Ce6 binding to AuNPs.

## Conclusions

New method of synthesis of hybrid nanosystems in branched water-soluble polymer matrix based on the branched copolymers dextran–polyacrylamide in nonionic and anionic form with incorporated gold nanoparticles and photosensitizer chlorin e6 has been developed. The nanocomposites were characterized by TEM, DLS and UV–visible spectroscopy. It was shown that nanocomposites were stable in time and contained AuNPs of 10–20 nm in size.
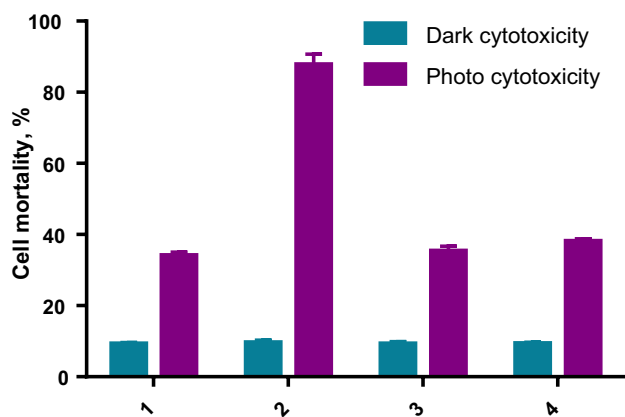
**Fig. 8** Dark cytotoxicity and photodynamic activity of D-*g*-PAA(PE)/AuNPs/Ce6 nanosystems with different $HAuCl_4$:$NaBH_4$ mass ratios during their synthesis. 1—Ce6 alone; 2—$HAuCl_4$:$NaBH_4$ mass ratio 1:2; 3—$HAuCl_4$:$NaBH_4$ mass ratio 1:4; 4—$HAuCl_4$:$NaBH_4$ mass ratio 1:6

Analysis of absorption spectra of nanosystems D70-*g*-PAA/AuNPs/Ce6 and D70-*g*-PAA(PE)/AuNPs/Ce6 demonstrated that the efficiency of Ce6 decreases more slowly with increasing of AuNPs concentration for nanosystem synthesized in anionic polymer matrix.

It was established that neither the dextran–polyacrylamide copolymer nor the system of "polymer/AuNPs" independently produce singlet oxygen for the parameters of laser irradiation used for photodynamic damage to cells. The gradual decrease of singlet oxygen production with the rise of Au content in nanocomposites D-*g*-PAA(PE)/AuNPs/Ce6 for all doses of laser irradiation applied was observed. However, for the nanocomposite with the Ce6:Au mass ratio 1:10 $^1O_2$ generation of singlet was quite close to that for free Ce6. The ability of this nanosystem to sensitize MT-4 cells to photodynamic damage was tested. It was shown that the nanocomposite, which contained AuNPs during the synthesis of which $HAuCl_4$:$NaBH_4$ mass ratio was 1:2, showed higher photodynamic activity, than Ce6 itself.

On the base on the complex analysis of the triple system with different types of polymer, it was concluded that nanosystem D70-*g*-PAA(PE)/AuNPs/Ce6 can be recommended to experiment in vivo.

# References

Abbas M, Zou Q, Li Sh, Yan X (2017) Self-assembled peptide- and protein-based nanomaterials for antitumor photodynamic and photothermal therapy. Adv Mater. https://doi.org/10.1002/adma.201605021

Bauer G (2016) The antitumor effect of singlet oxygen. Anticancer Res 36:5649–5664. https://doi.org/10.21873/anticanres.11148

Bauer G (2017) Autoamplificatory singlet oxygen generation sensitizes tumor cells for intercellular apoptosis-inducing signaling. Mech Ageing Dev. https://doi.org/10.1016/j.mad.2017.11.005

Boué F, Combet J, Demé B, Heinrich M, Zilliox JG, Rawiso M (2016) SANS from salt-free aqueous solutions of hydrophilic and highly charged star-branched polyelectrolytes. Polymers 8:228. https://doi.org/10.3390/polym8060228

Cai W, Gao T, Hong H, Sun J (2008) Applications of gold nanoparticles in cancer nanotechnology. Nanotechnol Sci Appl. 1:17–32. https://doi.org/10.2147/NSA.S3788

Castano AP, Demidova TN, Hamblin NR (2004) Mechanisms in photodynamic therapy: part one—photosensitizers, photochemistry and cellular localization. Photodiagn Photodyn Ther 1(4):279–293. https://doi.org/10.1016/S1572-1000(05)00007-4

Charrueau C, Zandanel C (2016) Drug delivery by polymer nanoparticles: the challenge of controlled release and evaluation. In: Vauthier C, Ponchel G (eds) Polymer nanoparticles for nanomedicines. Springer, Cham. https://doi.org/10.1007/978-3-319-41421-8_14

Chithrani DB, Jelveh S, Jalali F, van Prooijen M, Allen Ch, Bristow G, Hill RP, Jaffray DA (2010) Gold nanoparticles as radiation sensitizers in cancer therapy. Radiat Res 173(6):719–728. https://doi.org/10.1667/RR1984.1

Dougherty TJ (1977) Phototherapy of human tumors. In: Castellani A (ed) Research in photobiology. Plenum Press, New York, pp 435–446. https://doi.org/10.1111/j.1751-1097.1993.tb04990.x

Dougherty TJ, Kaufman J, Goldfarb A et al (1978) Photoradiation therapy for the treatment of malignant tumors. Cancer Res. 38:2628–2635 **(PubMed 667856)**

Everaers R, Grosberg AY, Rubinstein M, Rosa A (2017) Flory theory of randomly branched polymers. Soft Matter 13(6):1223–1234. https://doi.org/10.1039/c6sm02756c

Gladkova OL, Parkhats MV, Gorbachova AN, Terekhov SN (2010) FTIR spectra and normal-mode analysis of chlorine 6 and its degradation-induced impurities. Spectrochim Acta A 76:388–394. https://doi.org/10.1016/j.saa.2010.03.037

Kutsevol N, Bezugla T, Bezuglyi M, Rawiso M (2012) Branched dextran-graft-polyacrylamide copolymers as perspective materials for nanotechnology. Macromol Symp 317–318(1):82–90. https://doi.org/10.1002/masy.201100087

Kutsevol N, Bezuglyi M, Rawiso M, Bezugla T (2014) Star-like dextran-graft-(polyacrylamide-*co*-polyacrylic acid) copolymers. Macromol Symp 335:12–16. https://doi.org/10.1002/masy.201200115

Kutsevol NV, Chumachenko VA, Rawiso M, Shkodich VF, Stoyanov OV (2015) Star-like polymers dextran–polyacrylamide: the prospects of application for nanotechnology. Journal of structural chemistry 56(5):1016–1023. https://doi.org/10.15372/JSC20150521

Liu Y et al (2017) Water-insoluble photosensitizer nanocolloids stabilized by supramolecular interfacial assembly towards photodynamic therapy. Scientific Reports (7). https://doi.org/10.1038/srep4297

Merlitz H, Wu CH, Sommer JU (2011) Starlike Polymer Brushes. Macromolecules 44(17):7043–7049. https://doi.org/10.1021/ma201363u

Riethmuller M, Burger N, Bauer G (2015) Singlet oxygen treatment of tumor cells triggers extracellular singlet oxygen generation, catalase inactivation and reactivation of intercellular apoptosis-inducing signaling. Redox Biol 6:157–168. https://doi.org/10.1016/j.redox.2015.07.006

Shroff K, Vidyasagar A (2013) Polymer nanoparticles: newer strategies towards targeted cancer therapy. J Phys Chem Biophys 3:125. https://doi.org/10.4172/2161-0398.1000125

Solano-Umaña V, Vega-Baudrit JR (2015) Gold and silver nanotechnology on medicine. J Chem Biochem 3(1):21–33. https://doi.org/10.15640/jcb.v3n1a2

Song J, Xing R, Jiao T, Peng Q, Yuan C, Möhwald H, Yan X (2017) Crystalline dipeptide nanobelts based on solid-solid phase transformation self-assembly and their polarization imaging of cells. ACS Appl Mater Interfaces. https://doi.org/10.1021/acsami.7b17933

Triesscheijn M, Baasa P, Schellensa JHM, Stewart FA (2006) Photodynamic therapy in oncology. Oncologist 11(9):1034–1044. https://doi.org/10.1634/theoncologist.11-9-1034

Wang H, Rempel GL (2015) Introduction of polymer nanoparticles for drug delivery applications. J Nanotechnol Nanomed Nanobiotechnol 2:008. https://doi.org/10.24966/NTMB-2044/100008

Xing R, Liu K, Jiao T, Zhang N, Ma K, Zhang R, Zou Q, Ma G, Yan X (2016) An injectable self-assembling collagen–gold hybrid hydrogel for combinatorial antitumor photothermal/photodynamic therapy. Adv Mater 28:3669–3676. https://doi.org/10.1002/adma.201600284

Yang Y, Liu H, Han M, Sun B, Li J (2016) Multilayer microcapsules for FRET analysis and two-photonactivated photodynamic therapy. Angew Chem Int Ed 55:1–7. https://doi.org/10.1002/anie.201605905

Yeshchenko OA, Kutsevol NV, Naumenko AP (2016) Light-induced heating of gold nanoparticles in colloidal solution: dependence on detuning from surface plasmon resonance. Plasmonics 11(1):345–350. https://doi.org/10.1007/s11468-015-0034-z

Zenkevich E, Sagun E, Knyukshto V, Shulga A, Mironov A, Efremova O, Bonnett R, Songca SP, Kassem M (1996) Photophysical and photochemical properties of potential porphyrin and chlorin photosensitizers for PDT/E. J Photochem Photobiol B 33:171–180. https://doi.org/10.1016/1011-1344(95)07241-1

Zhang R, Xing R, Jiao T-F, Ma K, Chen C, Ma G, Yan X (2016) Carrier-free, chemo-photodynamic dual nanodrugs via self-assembly for synergistic antitumor therapy. ACS Appl Mater Interfaces. https://doi.org/10.1021/acsami.6b02416